

SENSORLESS SPEED AND REACTIVE POWER CONTROL OF A DFIG-WIND TURBINE

¹ADIL BARRA, ²HAMID OUADI

^{1,2} PMMAT Lab, University Hassan II, Faculty of Science, Casablanca, Morocco

E-mail: barra.adil@gmail.com, hamidouadi3@yahoo.fr

ABSTRACT

This paper deals with the problem of wind turbine – DFIG (doubly fed induction generator) speed control. For energy optimization purpose, several optimal wind-turbine speed control strategies have been proposed. However, these techniques require the measurement of wind speed and rotor speed which are both difficult in practice and not very reliable. In this work, sensorless maximum power point tracking (MPPT) control is developed. The control objective is twofold: (i) tracking the maximum available wind power; (ii) regulating the DFIG reactive power. The rotor speed and wind speed are estimated using a nonlinear observer based on the state space model representing the whole DFIG-wind turbine. Moreover, using the estimated mechanical variables, a nonlinear control law is developed with the sliding mode technical to achieve the control objective. The performances of the proposed regulator are analyzed using tools from the Lyapunov stability. These theoretical results are validated by simulation with a wide variation of the wind speed.

Keywords: *DFIG, MPPT, Sliding Mode, High Gain Observer, Lyapunov Stability.*

1. INTRODUCTION

The electrical energy producing from wind turbine is an economic and own alternative relatively to various exhaustible energy sources [1]. In this context, this paper deals with the problem of the wind turbine speed control. The considered generator is a doubly fed induction (DFIG). The rotor is connected to the power grid through an AC-DC-AC converter, while the stator is directly connected to the network (see Figure 1). The fundamental advantage of this arrangement is that the power flowing through the converter is only a fraction of the total wind turbine power. Therefore its size, cost and losses are much smaller compared to a full-scale power converter placed on the stator. To maximize the wind energy extraction, variable wind turbine speed control (MPPT), were proposed. This technique requires the knowledge of the wind speed, and consists in varying the turbine speed reference according to that of the wind [2]. Several

MPPT regulators have been developed to control the DFIG through the rotor. However, most previous works have been devoted to the simple case considering that the wind speed is available by using physical sensors [3]. The point is that physical sensors raise several practical problems of robustness, maintenance, cost and precision.

To avoid this difficulty, some previous works propose sensorless MPPT wind turbine control [4]-[5]. Various models have been proposed for estimating wind speed. One can distinguishes frequency models, statistical or even autoregressive models [6]. The proposed estimators generally lead to complex computations and so, raise practical problems of real time implementation. Other studies estimate the wind speed as well as the aerodynamic torque by using a state observer based on a linearized model of the wind turbine [7]. The observer performances are guaranteed only in a neighborhood of an operating point.

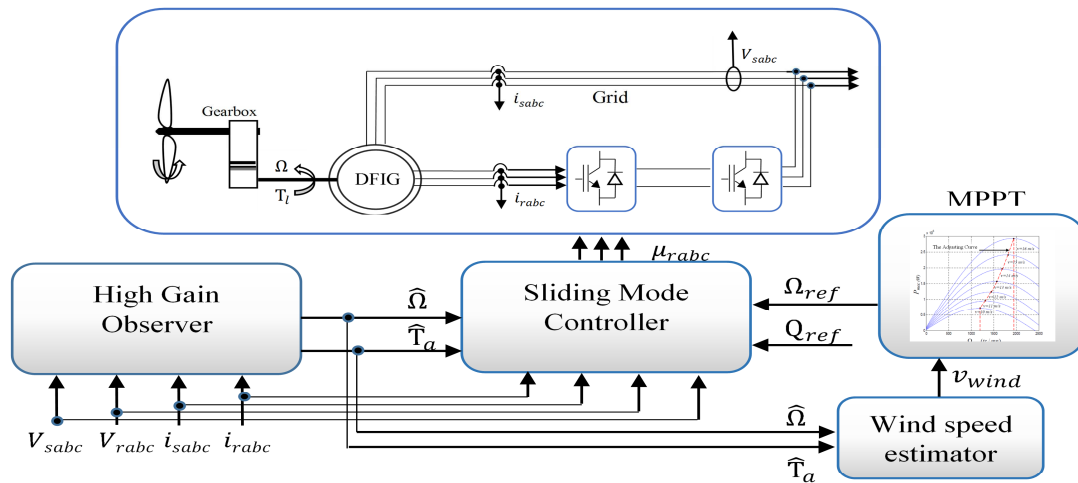


Fig. 1. Wind turbine system architecture considered.

In the other hand, different techniques have been used to design the MPPT control law. In [8], a simple linear controller is proposed. However, for systems such as DFIG-wind turbine, which enjoys non-linear dynamics, the performance of such regulator degrades during wide variations of wind speed. Also neural, fuzzy or hysteresis methods are used to design the wind turbine control system [8]-[9]. However, those techniques do not make use of the exact nonlinear DFIG-wind turbine model in the control design. Consequently, the obtained controllers are generally not backed by formal stability analysis and their performances cannot be expressly quantified.

In this paper, sensorless MPPT control of DFIG is proposed. The control objective is twofold: (i) tracking the maximum available wind power; (ii) regulating the DFIG reactive power. The rotor speed, aerodynamic torque and wind speed are estimated using a nonlinear observer based on the state space model representing the whole DFIG-wind turbine. Moreover, using the estimated mechanical variables, a nonlinear control law is developed with the sliding mode technical to achieve the control objective.

The performances of the proposed regulator are analyzed using tools from the Lyapunov stability. These theoretical results are validated by simulation with a wide variation of the wind speed.

The paper is organized as follows: The wind turbine model is presented in Section II. Section III is devoted to the rotor speed aerodynamic torque and wind speed estimation. The controller synthesis is discussed in section IV. The estimator and the control law performances are illustrated by

simulation in Section V, a conclusion and reference list end the paper.

2. WIND TURBINE MODEL

In this section we present the wind turbine model for the MPPT control with rotor speed regulation. Fig. 1 shows the overall architecture of the wind energy conversion system considered. The involved notations are described in Table 1.

Table 1. Notations and symbols

p	poles pairs		
Ω, ω_r	DFIG rotor speed	rad/s	$(\omega_r = p\Omega)$
V_{sd}, V_{sq}	Stator voltage components	(d-q)	V
V_{rd}, V_{rq}	Rotor voltage components	(d-q)	V
P_a	Aerodynamic power		W
J	Total inertia constant		Kg.m ²
L_s, L_r	Stator, Rotor cyclic induction		H
M_{sr}	Mutual cyclic induction		H
R_s, R_r	Stator, Rotor resistance (per phase)		Ω
ω_s	Stator pulsation		rad/s
i_{rd}, i_{rq}	Rotor current components	(d-q)	A
i_{sd}, i_{sq}	Stator current components	(d-q)	A
T_a	Aerodynamic Torque		N.m
v	Wind speed		m/s
R	Rotor radius		m
$C_p(\lambda)$	Power coefficient		
λ	Tip-speed ratio		



ρ	Air density	Kg/m ³
σ	Dispersion ratio	
F	Friction ratio	

2.1. Turbine Model

The available aerodynamic wind power is given by [10]:

$$P_a = \frac{1}{2} \rho \pi R^2 C_p(\lambda) v^3 \tag{1}$$

where the tip speed ratio λ is given by:

$$v = \frac{R \cdot \Omega}{\lambda} \tag{2}$$

2.2. DFIG Control Model

The model considered for DFIG is a state model widely used in the literature. It is developed in a rotating reference frame (d-q) [6] as follows:

$$\begin{bmatrix} \dot{i}_{sd} \\ \dot{i}_{sq} \\ \dot{i}_{rd} \\ \dot{i}_{rq} \\ \dot{\Omega} \\ \dot{T}_a \end{bmatrix} = \begin{bmatrix} aV_{sd} - bV_{rd} - ci_{sd} + di_{rd} + l(\omega_s - \omega_r)i_{rq} + \frac{1}{\sigma}(\omega_s - f\omega_r)i_{sq} \\ aV_{sq} - bV_{rq} - ci_{sq} + di_{rq} - l(\omega_s - \omega_r)i_{rd} - \frac{1}{\sigma}(\omega_s - f\omega_r)i_{sd} \\ gV_{rd} - bV_{sd} - Hi_{rd} + Ii_{sd} - j(\omega_s - \omega_r)i_{sq} - \frac{1}{\sigma}(f\omega_s - \omega_r)i_{rq} \\ gV_{rq} - bV_{sq} - Hi_{rq} + Ii_{sq} + j(\omega_s - \omega_r)i_{sd} + \frac{1}{\sigma}(f\omega_s - \omega_r)i_{rd} \\ -C \cdot \Omega + m(i_{rq}i_{sd} - i_{rd}i_{sq}) - \frac{T_a}{J} \\ 0 \end{bmatrix} \tag{3}$$

where the state space vector and the control vector considered are respectively:

$$X = [x_1 \ x_2 \ x_3 \ x_4 \ x_5 \ x_6]^T = [i_{sd} \ i_{sq} \ \Omega \ T_a \ i_{rd} \ i_{rq}]^T \tag{4}$$

$$u = [V_{rd} \ V_{rq}]^T. \tag{5}$$

The model parameters are defined in Table 2

a	$\frac{1}{(\sigma \cdot L_s)}$	g	$\frac{1}{(\sigma \cdot L_r)}$
b	$\frac{M_{sr}}{\sigma \cdot L_r L_s}$	H	$\frac{R_r}{\sigma L_r}$
c	$\frac{R_s}{\sigma L_s}$	I	$\frac{R_s M_{sr}}{\sigma \cdot L_r L_s}$
d	$\frac{R_r M_{sr}}{\sigma \cdot L_r L_s}$	j	$\frac{M_{sr}}{\sigma L_r}$
l	$\frac{M_{sr}}{\sigma L_s}$	σ	$1 - \frac{M_{sr}^2}{L_r L_s}$
f	$\frac{M_{sr}^2}{L_r L_s}$	C	$\frac{F}{J}$
m	$-\frac{p M_{sr}}{J}$		

3. OBSERVER DESIGN

Variable wind turbine speed control requires the knowledge of the wind speed, rotor speed and aerodynamic torque. The use of physical sensors raises several practical problems of robustness, maintenance, cost and precision. In this section,

based on the DFIG-turbine model (1)-(3) a new observer is designed for the aerodynamic torque and wind turbine speed. The estimation of these two variables is then used for determination of the wind speed.

3.1. DFIG Observer

As suggested in [11], the DFIG model (3) is rewriting in the following form:

$$\dot{x} = A(s)x + G(u, s, x) \tag{6}$$

$$y = C_y x \tag{7}$$

where:

- x is the reduced state space vector defined by $x = [x_1 \ x_2 \ x_3 \ x_4]^T = [i_{sd} \ i_{sq} \ \Omega \ T_a]^T$ (8a)
- $y = [i_{sd} \ i_{sq}]^T$ is the output vector. (8b)
- $C_y = [1 \ 1 \ 0 \ 0]$ is the output matrix. (8c)
- s includes variables considered as measurable quantity defined by: $s = [V_{sd} \ V_{sq} \ i_{rd} \ i_{rq}]^T$ (8d)

and

$$A(s) = \begin{bmatrix} 0_2 & F_1(s) \\ 0_2 & 0_2 \end{bmatrix}; \tag{9}$$

$$F_1(s) = \begin{bmatrix} l p \ i_{rq} + \frac{f p}{\sigma} i_{sq} & 1 \\ -l p \ i_{rd} - \frac{f p}{\sigma} i_{sd} & 1 \end{bmatrix}$$

$$G(u, s, x) = \begin{bmatrix} aV_{sd} - bV_{rd} - ci_{sd} + di_{rd} + \frac{1}{\sigma}(1-f)\omega_s i_{sq} - T_a \\ aV_{sq} - bV_{rq} - ci_{sq} + di_{rq} + \frac{1}{\sigma}(1-f)\omega_s i_{sd} - T_a \\ m(i_{rq}i_{sd} - i_{rd}i_{sq}) - \frac{T_a}{J} - C\Omega \\ 0 \end{bmatrix} \tag{10}$$

with the above notations, the proposed observer can simply be formulated as follows:

$$\hat{\dot{x}} = A(s)\hat{x} + \hat{G}(u, s, y) + M(y, s)C_y \tilde{x} \tag{11}$$

where

$$\hat{G}(u, s, y) = \begin{bmatrix} aV_{sd} - bV_{rd} - ci_{sd} + di_{rd} + \frac{1}{\sigma}(1-f)\omega_s i_{sq} \\ aV_{sq} - bV_{rq} - ci_{sq} + di_{rq} + \frac{1}{\sigma}(1-f)\omega_s i_{sd} \\ m(i_{rq}i_{sd} - i_{rd}i_{sq}) \\ 0 \end{bmatrix} \tag{12}$$

The aim of observer analysis is to perform a suitable choice of the observer gain $M(y)$. This is the subject of the next theorem, where the following notations are used:



$$\Delta_\theta = \begin{bmatrix} 1 & 0 & 0 & 0 \\ 0 & 1 & 0 & 0 \\ 0 & 0 & \frac{1}{\theta} & 0 \\ 0 & 0 & 0 & \frac{1}{\theta^2} \end{bmatrix}; K = \begin{bmatrix} K_1 \\ K_1 \\ K_2 \\ K_2 \end{bmatrix}; \Gamma(s) = \begin{bmatrix} I_2 & O_2 \\ O_2 & F_1(s) \end{bmatrix} \quad (13)$$

$$\bar{A} = \begin{bmatrix} O_2 & I_2 \\ O_2 & O_2 \end{bmatrix}; C_1 = C_y \Gamma^{-1}(s) \Delta_\theta^{-1} \text{ and } \bar{A} = (\bar{A} - K C_1) \quad (14)$$

where θ, K_1, K_2 are positives real parameters. Notice that Δ_θ and Γ are invertible.

3.3. Observer Analysis

Let us introduce the following estimation error:

$$\tilde{x} = x - \hat{x} \quad (15)$$

using (6) and (11), time derivative for the estimation error is given by:

$$\dot{\tilde{x}} = (A - M(s)C_y)\tilde{x} + \Lambda(T_a, \Omega) \quad (16)$$

where

$$\Lambda = \begin{bmatrix} -T_a & -T_a & \left(\frac{-T_a}{J} - c\Omega\right) & 0 \end{bmatrix}^T \quad (17)$$

Let us introduce the following modified error variable:

$$e = \Gamma(s)\Delta_\theta \tilde{x} \quad (18)$$

Then it follows from (18), using (16) that:

$$\dot{e} = \dot{\Gamma}(s)\Gamma^{-1}(s)e + \Gamma(s)\Delta_\theta(A - M(s)C_y)\Delta_\theta^{-1}\Gamma^{-1}(s)e + \Gamma(s)\Delta_\theta \Lambda(T_a, \Omega) \quad (19)$$

To analyze the stability of the error system (19), consider the Lyapunov function candidate defined by:

$$V = e^T P e \quad (20)$$

where P is a symmetric positive definite matrix satisfying the following equation:

$$\bar{A}^T P + P \bar{A} = -P \quad (21)$$

Theorem.1

Consider the DFIG representing by model (3) and assume that the rotor speed, the aerodynamic torque, the measurable quantity vector $s = [V_{sd} V_{sq} i_{ra} i_{rq}]^T$ and its time-derivative remain bounded. To estimate the reduced state vector x , consider the observer (11)-(12) with the matrix gain $M(s)$ of the form:

$$M(s) = \Gamma^{-1}(s)\Delta_\theta^{-1}K \quad (22)$$

and let the parameter θ in (22) be chosen such that:

$$\theta > 2\lambda_{min}^{-1} L_{\Gamma\Gamma^{-1}} \|P\| \quad (23)$$

where $L_{\Gamma\Gamma^{-1}} = \sup \|\dot{\Gamma}(s)\Gamma^{-1}(s)\|$ and λ_{min} the smallest value of matrix P

Then, one has the following results:

- The observation error system (15) is globally stable.
- The larger the parameter θ , the smaller the norm of the estimation error vector $\tilde{x} = [\tilde{i}_{sd} \tilde{i}_{sq} \tilde{\omega} \tilde{T}_a]^T$

Proof of Theorem.1

Substituting (22) in (19), with notation (14), one has

$$\dot{e} = \dot{\Gamma}(s)\Gamma^{-1}(s)e + \theta \bar{A}e + \Gamma \Delta_\theta \Lambda \quad (25)$$

Then, using (25) and (21), time derivative of the Lyapunov function candidate (20) is given by:

$$\dot{V} = -\theta V + 2e^T P \dot{\Gamma}(s)\Gamma^{-1}(s)e + 2e^T P \Gamma(s)\Delta_\theta \Lambda(T_a, \Omega) \quad (26)$$

with (26), one can have the inequality:

$$\dot{V} \leq -\theta V + 2\|e^T P \dot{\Gamma}(s)\Gamma^{-1}(s)e\| + 2\|e^T P \Gamma(s)\Delta_\theta \Lambda(T_a, \Omega)\| \quad (27)$$

Let's set

$$L_\Gamma = \sup \|\Gamma(s)\| \quad (28)$$

λ_{max} = Largest value of definite positive matrix P (21)

$L_\Lambda = \sup(\Lambda(T_a, \Omega))$: L_Λ exists because aerodynamic torque and rotor speed are assumed to be bounded.

Then with (27) one has:

$$\dot{V} \leq -aV + b\sqrt{V} \quad (29)$$

where

$$a = \theta - 2\lambda_{min}^{-1} L_{\Gamma\Gamma^{-1}} \|P\| \quad (30)$$

$$b = 2L_\Lambda L_\Gamma \|P\| \lambda_{min}^{-0.5} \quad (31)$$

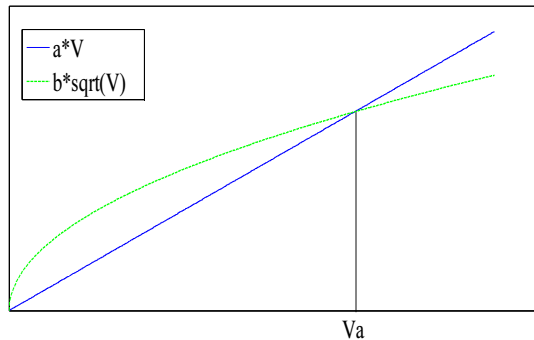


Fig. 2. The shape of the functions $g_1(\cdot)$ and $g_2(\cdot)$ versus V

Let us introduce the functions $g_1(V) = aV$ and $g_2(V) = b\sqrt{V}$. These are represented by Fig 2. This figure, together with (29), shows that the value of $V(t)$ will converge to the interval $[0, V_A]$ whatever its initial value $V(0)$. Where V_A is the solution of the equation $g_1(V) = g_2(V)$, given by:

$$V_A = \left(\frac{b}{a}\right)^2 \quad (32a)$$

This proves Part 1 of the Theorem. Furthermore, it follows from (30)-(31) that:

$$V_A = \left(\frac{2L_{\wedge}L_{\Gamma}\|P\|\lambda_{min}^{-0.5}}{\theta - 2\lambda_{min}^{-1}L_{\Gamma}^{-1}\|P\|}\right)^2 \quad (32b)$$

which clearly shows that V_A is a decreasing function of the parameter θ . Then, the larger θ is the smaller V_A (and consequently the smaller the norm of the error). This ends the proof of the Theorem ■

3.3 Wind Speed Computation

The objective of this subsection is to determine the wind speed from the estimation of the aerodynamic torque and rotor speed.

From the turbine model (1)-(2), tip speed ratio estimation $\hat{\lambda}$ is the solution of the non linear equation given by:

$$C_p(\hat{\lambda}) = 2 \frac{\hat{T}_a \hat{\lambda}^3}{\rho \pi R^5 \hat{\Omega}^2} \quad (33)$$

Recall that the general shape of C_p versus λ is represented in figure (3), (see e.g. [10]).

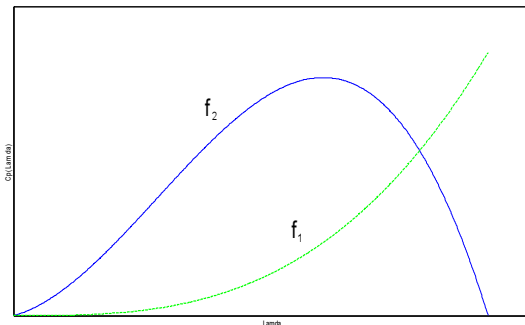


Fig. 3. Solid line: General shape of $C_p(\lambda)$. Dotted line: Evolution of the right side of equation (33), versus λ .

Fig. 3 shows that for a given value of \hat{T}_a and $\hat{\Omega}$, equation (33) presents a unique solution ($\hat{\lambda}$). Now, with the estimated tip speed ratio, one can easily deduce (using (2)), the wind speed estimation:

$$\hat{v} = \frac{R \cdot \hat{\Omega}}{\hat{\lambda}} \quad (34)$$

4. CONTROLLER DESIGN

Recall that the control objective is twofold: (i) tracking the maximum available wind power, with a variable turbine speed control (ii) regulating the DFIG reactive power. The rotor speed and wind speed are estimated using a nonlinear observer described above. The control law is developed using the sliding mode technical. The general structure of the proposed controller is described in Fig. 4.

The sliding surface considered is defined by

$$S = \begin{bmatrix} S_1 \\ S_2 \end{bmatrix} = \begin{bmatrix} k_1 \int e_1 + e_1 \\ k_2 \int e_2 + e_2 \end{bmatrix} \quad (35)$$

with:

$$e_1 = \hat{\Omega} - \Omega_{ref} \quad (36)$$

$$e_2 = Q - Q_{ref} \quad (37)$$

where references signals Ω_{ref} and Q_{ref} are considered, continuous, bounded and twice time differentiable. Their first and second derivatives are also bounded. Moreover, the observer dynamic is considered to be very fast compared to the controller dynamic. This allowed during the control law synthesis, to confuse the estimated variables to their active value. The control synthesis is done in two steps:

First step: Using the DFIG model (3), the sliding surface dynamic is given by:

$$\dot{S} = F + D \begin{bmatrix} i_{rq} \\ V_{rd} \end{bmatrix} \quad (38)$$

where

$$D = \begin{bmatrix} -\mu \frac{V_s}{\omega_s} & 0 \\ 0 & -\frac{V_s M_{sr} g}{L_s} \end{bmatrix} \quad \text{and} \quad F = \begin{bmatrix} F_1 \\ F_2 \end{bmatrix} \quad (39)$$

with

$$F_1 = k_1(\hat{\Omega} - \Omega_{ref}) + (-C \cdot \hat{\Omega} - \frac{\hat{T}_a}{j} - \dot{\Omega}_{ref}) \quad (40)$$

$$F_2 = k_2 \left(\frac{V_s^2}{\omega_s L_s} - \frac{V_s M_{sr}}{L_s} i_{rd} - Q_{ref} \right) - \frac{V_s M_{sr}}{L_s} (-bV_{sd} - Hi_{rd} + I_{isd} - j(\omega_s - \hat{\omega}_r)i_{sq} - \frac{1}{\sigma}(f\omega_s - \hat{\omega}_r)i_{rq}) - \dot{Q}_{ref} \quad (41)$$

Equation (38) shows that sliding surface S can be controlled by the virtual vector input $[i_{sq} \ V_{rd}]^T$. In this first step, the objective is to determine the considered control vector for ensuring the attractiveness and invariance of the surface S = 0. Let's consider the Lyapunov function candidate:

$$V_s = \frac{1}{2} S^T S \quad (42)$$

Its time derivative is given by:

$$\dot{V}_s = S^T \cdot \dot{S} = S^T \cdot (F + D \cdot \begin{bmatrix} i_{rq} \\ V_{rd} \end{bmatrix}) \quad (43)$$

By choosing the virtual vector control such that:

$$\begin{bmatrix} i_{rq} \\ V_{rd} \end{bmatrix} = \begin{bmatrix} i_{eq} \\ V_{eq} \end{bmatrix} + \begin{bmatrix} i_{\tau} \\ V_{\tau} \end{bmatrix} = -D^{-1} F - D^{-1} \begin{bmatrix} d_1 \text{sign}(S_1) \\ d_2 \text{sign}(S_2) \end{bmatrix} \quad (44)$$

time derivative of the Lyapunov function candidate (42) becomes:

$$\dot{V}_s = -S^T \cdot \begin{bmatrix} d_1 \text{sign}(S_1) \\ d_2 \text{sign}(S_2) \end{bmatrix} \quad (45)$$

Equation (45), shows that $\dot{V}_s < 0$ ensuring the attractiveness of the sliding surface S = 0.

Noting that from (44), the d component of the control rotor voltage is given by:

$$V_{rd} = \frac{L_s}{V_s M_{sr} g} (F_2 + [d_2 \text{sign}(S_2)]) \quad (46)$$

Second step: The first step assumes that i_{rq} is the input control variable. Unfortunately, this is not the case in reality; we will then seek to reach asymptotically i_{rq} to I_{rqref} by acting on the real command V_{rq} . For this, we define the rotor current error e_i by:

$$e_i = i_{rq} - i_{rqref} \quad (47)$$

where i_{rqref} is deduced from (44) as

$$i_{rqref} = \frac{\omega_s}{\mu V_s} (F_1 + [d_1 \text{sign}(S_1)]) \quad (48)$$

Then using (48), (39) and the DFIG model (3), the rotor current error dynamic is given by:

$$\dot{e}_i = gV_{rq} + W_1 \quad (49)$$

where

$$W_1 = -bV_s - Hi_{rq} + I_{isq} + j(\omega_s - \hat{\omega}_r)i_{sd} + \frac{1}{\sigma}(f\omega_s - \hat{\omega}_r)i_{rd} - \frac{\omega_s}{\mu V_s} \left((k_1 - C)\hat{\Omega} - k_1 \dot{\Omega}_{ref} - \dot{\Omega}_{ref} + \left[d_1 \dot{S}_1 \cdot \frac{d \text{sign}(S_1)}{d S_1} \right] \right) \quad (50)$$

Then consider the extended Lyapunov function candidate:

$$V = V_s + \frac{1}{2} e_i^2 \quad (51)$$

Using (44), (43) and (49), time derivative of the Lyapunov function candidate V is given by:

$$\dot{V} = -S^T \left(\begin{bmatrix} d_1 \text{sign}(S_1) \\ d_2 \text{sign}(S_2) \end{bmatrix} \right) - \mu \frac{V_s}{\omega_s} S_1 e_i + e_i (gV_{rq} + W_1) \quad (52)$$

Equation (52) suggests the choice of the control input V_{rq} as:

$$V_{rq} = -\frac{1}{g} (W_1 + c_1 e_i - \mu \frac{V_s}{\omega_s} S_1) \quad (53)$$

Theorem 2

Consider the DFIG representing by (3). Consider the control law defined by (45), (53). Then, the rotor speed and reactive power errors defined respectively by (36) and (37) asymptotically vanish \square

Proof of Theorem.2

Introducing (53) in (52), time derivative of the Lyapunov function candidate becomes:

$$\dot{V} = -S_1 [d_1 \text{sign}(S_1)] - S_2 [d_2 \text{sign}(S_2)] - c_1 e_i^2 \quad (54)$$

This assures the global asymptotic stability of the tracking error system defined by (36-37, 47). This ends the proof of the Theorem \blacksquare

5. SIMULATIONS RESULTS

The simulations are performed on MATLAB / SIMULINK environment. The DFIG and Turbine parameters considered in this work are given in Table 3. The observer and the control law are implemented using equations (11)-(12), (22) and (45), (43) respectively. The corresponding design parameters are given the following numerical values of Table 4, which proved to be convenient. In this respect, note that there is no systematic way, especially in nonlinear control, to make suitable choices for these values. Therefore, the usual

practice consists in proceeding with trial-error approach. Doing so, the numerical values of Table 4 are retained. The whole simulated control system is illustrated by Fig. 5

Table.3.Electrical machine parameters.

Electrical	Index	Value
Stator resistance	R_s	0.455Ω
Rotor resistance	R_r	0.62Ω
Stator leakage inductance	L_s	0.0083H
Rotor leakage inductance	L_r	0.0081H
Magnetizing inductance	M_{sr}	0.0078H
Inertia	J	0.3125kgm ²
Viscous friction	F	6.73×10 ⁻¹ Nms ⁻¹

Table.4. Controller and Estimator parameters.

Index	Value	Index	Value
K_1	1	c_1	500
K_2	1	k_1	7000
d_1	0.0001	k_2	1000
d_2	0.1	θ	10000

The general shape of $C_p(\lambda)$ is presented in Fig.3. For the considered wind turbine, this curve was approximated with polynomial interpolation (see [12]) given by:

$$C_p(\lambda) = -0.2121\lambda^3 + 0.0856\lambda^2 + 0.2539\lambda \quad (55)$$

In the other hand, Fig 4 shows that for a given wind speed there exists a unique optimal rotor speed reference, for extracting the maximum mechanical power.

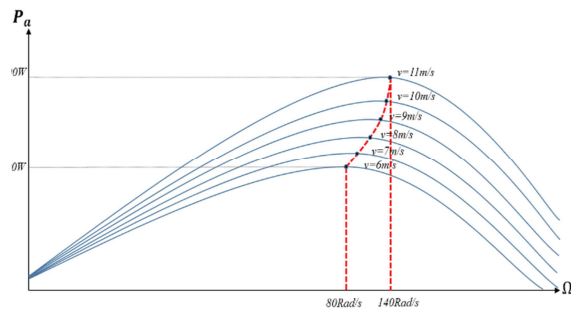


Fig. 4. Maximum power point tracking curves.

In this simulation, the optimal rotor speed reference curve (Ω_{ref} versus wind speed) was approximated with a polynomial interpolation (using the defined Matlab functions Polyfit, Polyval), given by:

$$\Omega_{ref} = -0.0011\hat{v}^4 + 0.0184\hat{v}^3 - 0.1644\hat{v}^2 + 0.7646\hat{v} - 1.4247 \quad (56)$$

5.1. Simulation Protocol

The simulation protocol is designed in such a way to consider a large step-variation of the mean wind speed (11.26 m/s – 6.34m/s: at time 0.2s (Fig. 6)). The resulting aerodynamic power is shown in Fig.7 and the corresponding optimal rotor speed

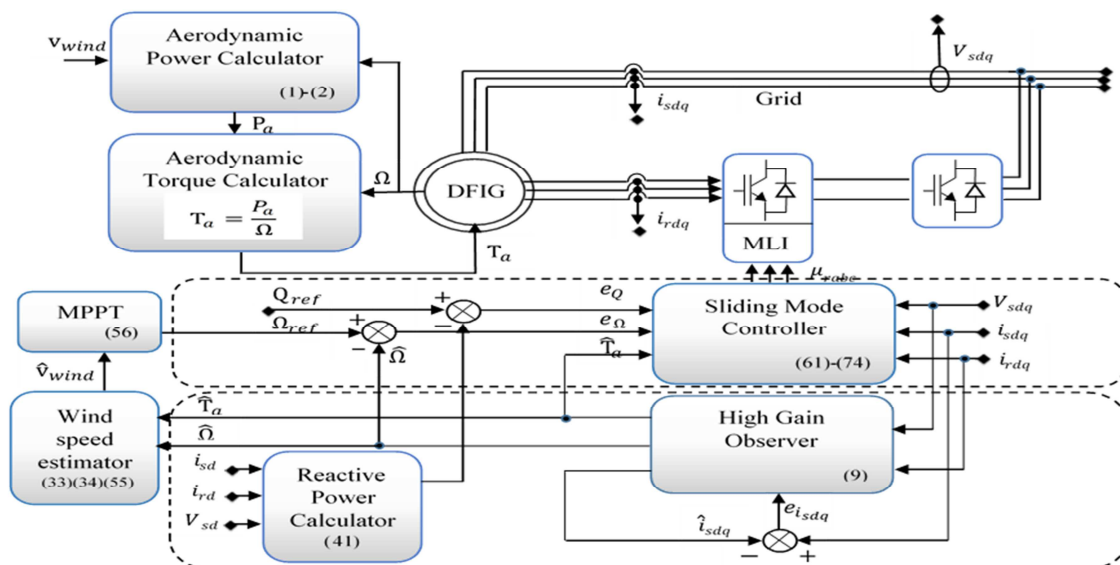


Fig. 5. Signals flow in the proposed Control-Observation strategy.

reference (determined by the MPPT algorithm) is represented in Solid line (Fig. 11). Similarly the DFIG reactive power reference signal considered is plotted in Solid line (Fig. 12). It also corresponds to a large step variation at time 0.1s.

(53). They show that the rotor speed and the reactive power track well their reference signal. Indeed, the corresponding tracking errors, also vanish

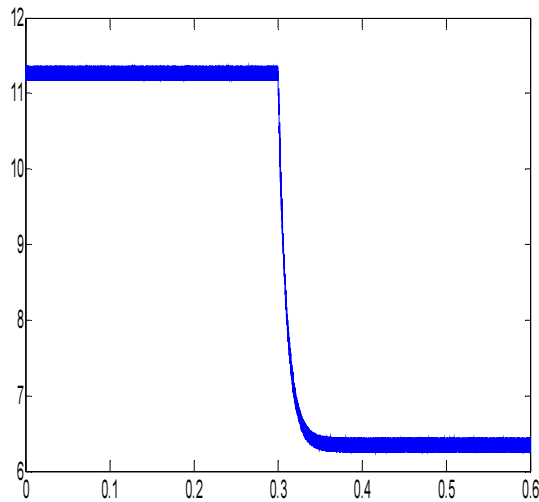


Fig. 6. The mean wind speed step-variation.

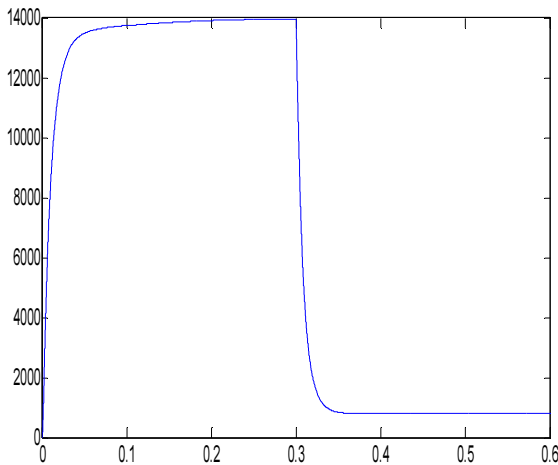


Fig. 7. Aerodynamic power.

5.2. Simulation Results

Fig. 8, Fig. 9 and Fig. 10 show the satisfactory performances of the observer. They confirm respectively that both estimated rotor speed, estimated aerodynamic torque and estimated wind speed track well their actual value.

Similarly, Fig. 11 and Fig. 12 show the satisfactory performances of the sensorless control law (46)-

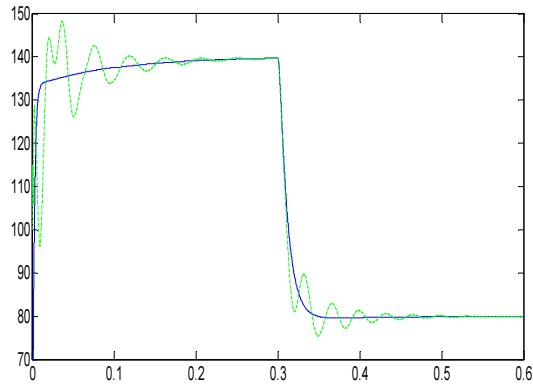


Fig. 8. Dotted line: Estimated rotor speed. Solid line: Its actual value.

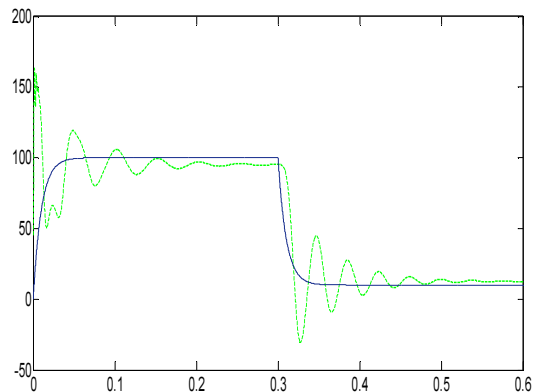


Fig. 9. Dotted line: Estimated aerodynamic torque. Solid line: Its actual value.

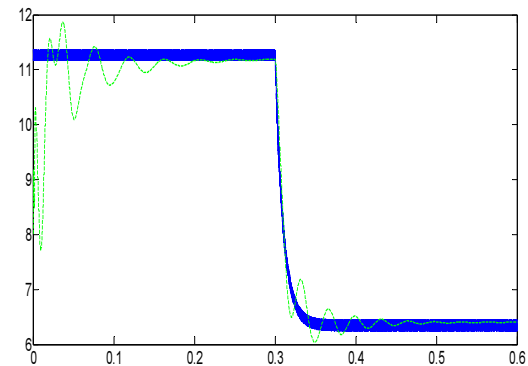


Fig. 10. Dotted line: Estimated wind speed. Solid line: Its actual value.

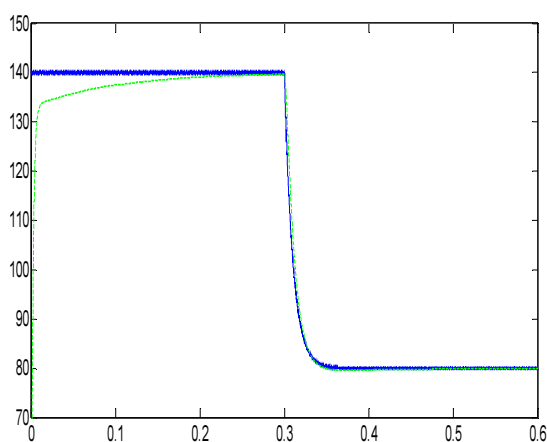


Fig.11. Dotted line: Wind turbine speed. Solid line: MPPT reference.

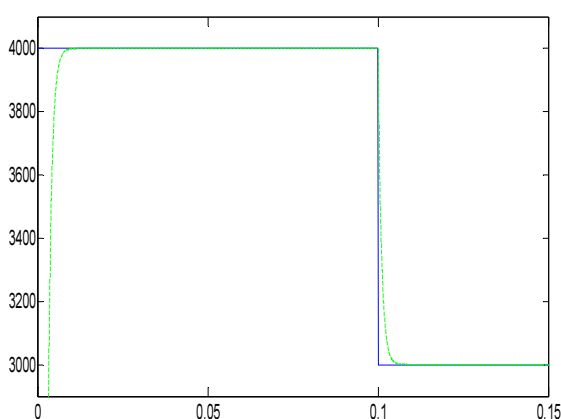


Fig.12. Dotted line: Reactive power. Solid line: Its reference.

6. CONCLUSION

This paper presents a sensorless MPPT control for wind turbine equipped with a DFIG. The aim is to achieve wind turbine speed and DFIG reactive power control. To this end, a nonlinear observer and controller are developed and analyzed making use of advanced tools from the control theory e.g. sliding mode control design, high gain observer. It is formally established that the control objectives are actually achieved with a quite satisfactory accuracy. The formal results are confirmed by simulations.

REFERENCES:

- [1] Marini, M., Capello, M., Goffi, M., Romei, G. (1998). "Technical and economical considerations about wind energy exploitation in the Ligurian area". *Journal of Wind Engineering and Industrial Aerodynamics*, Volumes 74–76, 1 April 1998, Pages 433–441.
- [2] Abdi, H., Hashemnia, N., Kashiha, A. (2011). "Active and reactive power control of a DFIG using a combination of VSC with PSO". *World Applied Sciences Journal*, 13(2), 316-323.
- [3] Beltran, B., Ahmed-Ali, T., and Benbouzid, M. E. (2008). "Sliding mode power control of variable-speed wind energy conversion systems", *IEEE Trans. Energy Conversion*, June.
- [4] Bezza, M., Moussaoui, B.E.L., Fakkar, A. (2012). "Sensorless MPPT Fuzzy Controller for DFIG Wind Turbine". *Energy Procedia*, Volume 18, (2012), Pages 339–348.
- [5] Boulahia, A., Nabti, K., Benalla, H. (2012). "Direct power control for ac/dc/ac converters in doubly fed induction generators based wind turbine". *Journal of Theoretical and Applied Information Technology (JATIT)*, 15 May 2012. Vol. 39 No.1.
- [6] Boukhezzar, B., Siguerdidjane, H. (2009). "Nonlinear control with wind estimation of a DFIG variable speed wind turbine for power capture optimization". *Energy Conversion and Management*, 50 (2009) 885–892.
- [7] Rocha, R. (2011). A sensorless control for a variable speed wind turbine operating at partial load. *Renewable Energy*, 36 (2011) 132-141.
- [8] Hamane, B., Benghanem, M., Bouzid, M. A., Belabbes, A., Bouhamida, M., Draou, A. (2012). "Control for Variable Speed Wind Turbine Driving a Doubly Fed Induction Generator using Fuzzy-PI Control". *Energy Procedia*, 18 (2012) 476 – 485.
- [9] Hilal, M., Errami, Y., Benchagra, M., Maaroufi, M. (2012). "Fuzzy power control for doubly fed induction generator based wind farm". *Journal of Theoretical and Applied Information Technology (JATIT)*, 30 September 2012. Vol. 43 No.2.
- [10] Soares, O., Gonçalves, H., Martins, A., Carvalho, A. (2010). "Nonlinear control of the doubly-fed induction generator in wind power systems". *Renewable Energy*, 35 (2010) 1662–1670.



- [11] Ouadi, H., Giri, F., De leon-morales, J., Dugard, L. (2005). "High-gain observer design for induction motor with nonlinear magnetic characteristic". *IFAC World congress, Prague, Czech July 4-8, 2005, Prague*.
- [12] Mirecki, A., Roboam, X., and Richardeau, F. (2007). "Architecture Complexity and Energy Efficiency of Small Wind Turbines". *IEEE transactions on industrial electronics*, vol. 54, no. 1, February 2007.